P4.1

RETRIEVAL OF WATER VAPOR OVER LAND SURFACES FROM MICROWAVE MEASUREMENTS

Alan E. Lipton*, Jean-Luc Moncet, John F. Galantowicz, and Jennifer D. Hegarty
Atmospheric and Environmental Research, Inc., Lexington, Massachusetts

1. INTRODUCTION

Current satellite-derived water vapor analysis products have substantial shortcomings with respect to spatial coverage. Infrared instruments have very limited capabilities in cloudy areas, where the radiative signatures of water vapor content may be largely shielded from view by the opacity of the intervening clouds. Microwave measurements are skillful in many cloudy conditions, but have had marginal skill over land surfaces. Operational applications of retrievals from microwave data from sensors such as SSM/I and AMSU have been largely confined to ocean areas, where microwave signatures of water vapor conditions are strongest. The difference in retrieval skill between ocean and land has been generally attributed to differences in surface emissivity and its stability over time, but the relative importance of various factors has not been thoroughly documented.

The sensitivity of microwave radiometric measurements to water vapor can be represented by the derivative with respect to water vapor amount in a layer, q_l, which can be approximated as

$$\frac{\partial T_B}{\partial q_l} = \frac{\partial T_B}{\partial \tau_l}\frac{\partial \tau_l}{\partial q_l} = \left(T_l - \varepsilon_s T_s\right)\Im_s \frac{\partial \tau_l}{\partial q_l},$$

where T_B is brightness temperature, T is temperature, τ is the optical depth of a layer, $\Im$ is the transmittance to space, s denotes the surface, and ε_s is the surface emissivity. The water vapor signal approaches zero whenever any of the terms on the right approach zero. The first term on the right is the contrast between the temperature of the layer and the effective temperature of the surface background. This term may be positive or negative, and may be small when $T_l \approx T_s$ and $\varepsilon_s \approx 1$, as is often the case over land surfaces.

Provided that a significant water vapor signal is present, the ability to accurately retrieve the water vapor content depends on how distinct is that signal in relation to signals that may arise from other environmental variables. If a certain change in water vapor content would cause the same change in brightness temperatures as a plausible change in surface type (emissivity), it is impossible to determine which change occurred, unless some prior information is available. This ambiguity can be relieved somewhat by making measurements at several frequencies, but only when the emissivities vary smoothly over frequency so there is a strong correlation between emissivity in a water vapor channel and other channels. It is particularly difficult to resolve the ambiguity between vapor and emissivity effect in cases where the vapor signal is weak.

2. EXPERIMENTAL APPROACH

2.1 *Retrieval Algorithm*

Retrieval experiments were performed to elucidate the importance of surface emissivity in the retrieval of water vapor and cloud parameters for clear and cloudy conditions. For convenience, we examined precipitable water (PW) and cloud liquid water (CLW), as they provide a good metric for the impact on water vapor and cloud retrievals, respectively. The algorithm used for the retrieval experiments is the physical inversion method that functions as the Core Module in the algorithm set for the Conical-scanning Microwave Imager/Sounder (CMIS), which is under development for the National Polar-orbiting Operational Environmental Satellite System (NPOESS).

Given a set of radiometric measurements of the atmosphere, the statistically most likely temperature profile is the one that minimizes the cost function

$$J(\mathbf{x}) = \left(\mathbf{y} - \mathbf{F}(\mathbf{x})\right)^T \mathbf{S}_y^{-1}\left(\mathbf{y} - \mathbf{F}(\mathbf{x})\right) + \left(\mathbf{x} - \mathbf{x}_0\right)^T \mathbf{S}_x^{-1}\left(\mathbf{x} - \mathbf{x}_0\right)$$

(Rodgers, 1976), where $\mathbf{x}$ is the atmospheric state vector that includes the temperature at discrete levels and may include other variables, $\mathbf{y}$ is a vector composed of the radiometric measurements, the operator $\mathbf{F}$ is a radiative transfer model that can be used to compute radiometric data from the state vector, and $\mathbf{x}_0$ is an *a priori* estimate of $\mathbf{x}$. The matrices $\mathbf{S}_y$ and $\mathbf{S}_x$ are the error covariances of the radiometric data and the *a priori* data, respectively. The matrix $\mathbf{S}_y$ represents data noise and errors in the radiative transfer model, and is generally taken to be diagonal. The retrieved state vector $\mathbf{x}$ is composed of the profiles of temperature and water vapor, the difference between skin surface temperature and surface air (shelter) temperature, the cloud liquid water, cloud top pressure and thickness, and the surface emissivity at the frequency of each of the channels.

In the CMIS algorithm, regularization is achieved by eigenvector transformations of the temperature profile, the water vapor profile, and the multichannel emissivities. Effectively, the algorithm retrieves the leading principal components of these variables, which are related to the original variables by a projection onto the leading eigenvectors of their respective covariance matrices. Those matrices are blocks along the diagonal of $\mathbf{S}_x$.

* *Corresponding author address*: Alan E. Lipton, Atmospheric and Environmental Research, Inc., 131 Hartwell Ave, Lexington, MA 02421; e-mail: alipton@aer.com

2.2 *Sensor Data*

The experiments were performed with simulated data from CMIS. The CMIS channel set is listed in Table 1. For these experiments, we used only the V and H-polarization channels at 18, 23, 36, and 89 GHz, 13 of the 60-GHz oxygen-band channels, and the water vapor channels near 166 and 183 GHz.

Table 1. CMIS channel set.

Channels[1]	Frequency Range (GHz)	Footprint Size (km)	EIA (°)
6V,H	6.45–6.8	68×40	55.7
10V,H,R,L	10.6–10.7	48×28	58.1
18V,H,P,M,R,L	18.6–18.8	24×15.5	53.6
23V,H	23.6–24.0	24×15.5	53.6
36V,H,P,M	36–37	18×12	55.7
60VX[2,3]	50.3–59.94	16×12	55.7
60LX[2,4]	60.371–60.509	16×12	55.7
60L FFT[5]	60.425–60.445	16×12	55.7
89V,H	87–91	16×12	55.7
166V[2]	166±0.7875	16×12	55.5
183VA-C[2]	183±0.71–±7.7	16×12	55.5

[1]Polarization: Vertical, Horizontal, Right- and Left-hand circular, P=+45°, M=-45°. [2]For sounding channel families, range of center frequencies is given. [3]X = A, B, C, D, E, F, G, J, and K. [4]X = L, M, U, and V. [5]FFT = Fast Fourier Transform receiver for upper atmosphere retrievals.

The CMIS channel set is similar to the conical-scanning SSMIS (Bommarito 1993), which is the successor to SSM/I and is scheduled to go operational in 2003. Some differences that are particularly relevant to this study are the SSMIS lack of an H-polarization channel near 23-GHz and its use of H polarization for sounding channels.

2.3 *Prior Information*

The constraints that stabilize the retrieval solution are represented by the *a priori* estimate of $\mathbf{x}$ (which is often called the background) and its error covariance. The atmosphere *a priori* statistics for CMIS are derived from a large database that represents global climatology. The land emissivity background is currently (during pre-launch development) derived from SSM/I observations (Prigent *et al*., 1997) in V and H polarization at 19, 37, and 85 GHz, by interpolation/extrapolation of surface emissivities to standard frequencies and to CMIS channels. The method used for interpolation to 23 GHz, in particular, is important for this study. We found experimentally that water vapor retrieval performance is significantly sensitive to the background correlation between the emissivities at 23 GHz and neighboring channels. When the correlation is higher, there are fewer independent unknowns for the algorithm to resolve, and the retrieval skill is higher. Effectively, the algorithm can get more water vapor information from the 23-GHz channel when the emissivity of the underlying surface can be precisely estimated from neighboring channels. In our data, the correlation was conservatively low because we applied random perturbations to the values obtained from linear interpolations and we checked that the spectral correlations were consistent with the source data.

2.4 *Analysis Method*

Tests were conducted for different types of land surfaces. We examined our emissivity data (Sec. 2.3) in relation to a surface type database and found that the emissivities depended heavily on vegetative cover. Our experiments focused on three surface types in particular (Table 2) that spanned a broad range of emissivities. Here, the typical emissivities are cited for 18/23 GHz at H polarization because those channels are spectrally near enough to have similar emissivities, even though they are not identical (Sec. 2.3).

Table 2. Typical H-polarization emissivity values for the three surface spectral emissivity types shown in Fig. 1 and Fig. 2.

Surface Type	18/23 GHz H-pol emissivity
Mixed Forest	0.94 – 0.96
Open Shrub	0.86 – 0.90
Barren/Sparse	0.80 – 0.86

The experiments also considered varying assumptions about the quality of *a priori* knowledge about the surface spectral emissivity. Improvement from a climatological constraint was modeled by adjusting the entire *a priori* emissivity spectrum from the climatological spectrum toward the "true" spectrum (test-case by test-case) using a scale factor. The square of the same scale factor was applied to the emissivity covariance matrix. As the scale factor was reduced from one experiment to the next, the effect was to simulate improved *a priori* emissivity knowledge. A convenient way to represent the overall quality of the *a priori* emissivity knowledge is with the standard deviation of the *a priori* error (the square-root of the covariance diagonal) at 18 and 23 GHz. That point in the emissivity spectrum is particularly important for vapor and cloud retrieval skill, as demonstrated below.

3. RESULTS

We examined PW and CLW retrieval performance in relation to a variety of parameters, and found that the dominant parameters were the emissivity characteristics at 18 and 23 GHz in H polarization. Fig. 1 and Fig. 2 show the retrieval errors as a function of the standard deviation of the 18 and 23 GHz emissivity background error for three surface spectral emissivity types, with the typical emissivity values for these types given in Table 1. The errors are root-mean-squares over a set of 400 test cases. An *a priori* emissivity standard deviation value of 0.12 corresponds to typical climatology, while smaller values model the increased knowledge provided by a recently updated, site-specific database. A value of 0.005 is expected for locations with very stable emissivity values, such as vegetated areas without recent precipitation. The magnitude of the decrease in retrieval error as the emissivity retrieval becomes more tightly constrained provides information about the sensitivity of the retrieved parameter to surface emissivity *a priori* knowledge. The scaling described above allowed us to explore the same range of background errors for each of the three surface types, although in nature a type with a higher emissivity tends to have a lower variability of that emissivity over time and space.

For PW and CLW, there is a strong dependence on emissivity (surface type) and the *a priori* emissivity knowledge. For cloudy sky regions the benefit of emissivity knowledge is diminished for PW for the surface with the highest emissivities (forest). For PW, improved *a priori* emissivity knowledge reduces the dependence of retrieval performance on 18/23 GHz emissivity (surface type), as is demonstrated by the convergence of the curves for smaller standard deviations. From another perspective, PW retrieval performance benefits most from having high-quality *a priori* emissivity data in areas where the emissivity is highest.

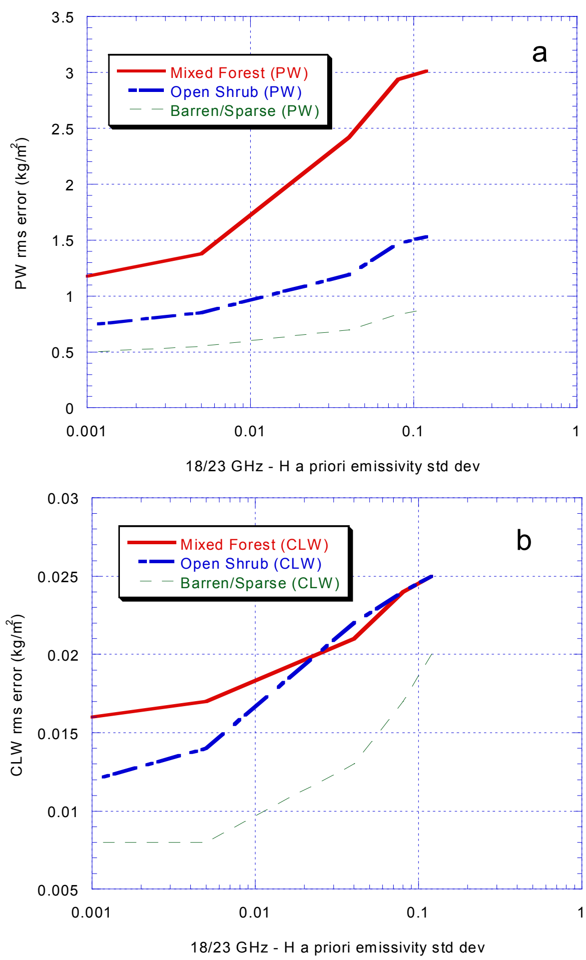

Fig. 1. Impact of *a priori* land surface emissivity information on clear sky retrievals of (a) precipitable water, and (b) cloud liquid water.

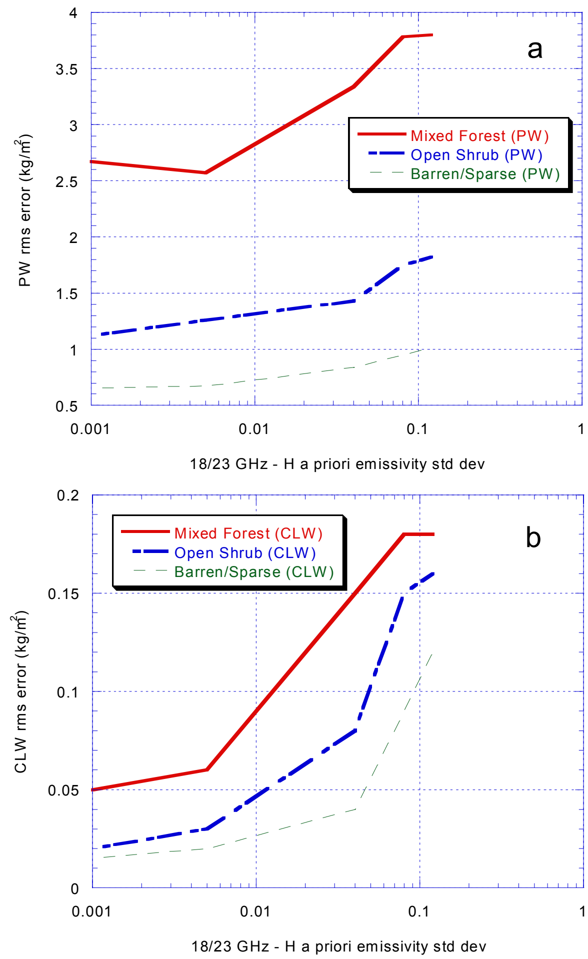

Fig. 2. Impact of *a priori* land surface emissivity information on cloudy sky retrievals of (a) precipitable water, and (b) cloud liquid water.

The dominance of the H-polarization 18/23-GHz emissivity among the factors affecting PW and CLW retrieval performance is rooted in radiometric sensitivity to water vapor. The water vapor line near 23 GHz provides strong sensitivity to lower-tropospheric water vapor, when a measurement on that line is analyzed in relation to neighboring window-channel measurements. The sensitivity to water vapor (and cloud) is maximized when the emissivity is lowest (Sec. 1). Emissivities of natural surfaces are typically lower in H polarization than in V.

4. SENSOR/ALGORITHM DESIGN IMPLICATIONS

A passive microwave sensor that has water vapor and cloud retrieval over land among its missions will be most effective if it includes a channel in H polarization at about 23 GHz. While the *a priori* variability (uncertainty) of the H-polarization emissivity is greater than for V, the H-polarization channel provides sensitivity that is not available with V-polarization alone. The SSMIS does not have such a channel. Cross-track scanners, such as AMSU, have a scan geometry that precludes measurement in a constant oblique angle and a fixed polarization and, therefore, they cannot benefit from the sensitivity available with a conical scanner in H polarization.

The CMIS algorithm design takes account of the findings of this study. For regions with stable emissivity values, a dynamic, localized emissivity database will be used to provide a better *a priori* estimate of the surface emissivity than would be provided by a climatological database. This dynamic database of day-to-day geo-located surface emissivity values will be derived from CMIS retrievals in conjunction with cross-sensor infrared data. Considering that emissivities can change suddenly, it is essential to test current measurements to see whether emissivities have departed from recent behavior, and to have alternative retrieval options depending on the degree of emissivity change.

In cases where a localized emissivity database is not available or the emissivity has not been stable, the CMIS algorithm employs pre-classification of scenes. The classification relies on a series of tests applied to brightness temperatures in channels 18H, 18V, 23H, 23V, 36V, and 89V. The tests were derived from the standing water test Neale et al. (1990) applied to SSM/I and a test for a scattering signature (Ferraro, et al., 1996). The classification skill benefits substantially from its adaptation to use the CMIS H-polarization measurement at 23 GHz.

The classifier is formulated and tuned specifically to identify scenes with high emissivity in the 18/23-GHz H channels. One reason for that focus is that it targets the classification to the cases where it can provide the greatest performance benefit. Another reason is system robustness. Any land scene not identified as having high 18/23-GHz-H emissivity has the “global” emissivity background constraint applied. The global background includes a broad variety of land surfaces, including wet land and high emissivity cases. By including high-emissivity cases in the global background, any high-emissivity retrieval scenes that the high-emissivity tests fail to detect will still use an acceptable background and will have acceptable retrieval performance. No attempt is made to pre-classify other surface types, such as scattering surfaces (desert, snow). There would be a substantial risk that a precipitating scene would be misclassified as a scattering surface, causing the Core Module to converge to an erroneous solution rather than generating a quality control flag that indicates possible precipitation contamination.

5. CONCLUSIONS

We show in this paper that the skill with which atmospheric water vapor (and cloud water amounts) can be retrieved over land is dominated by the surface emissivity near 23 GHz in particular and by the precision of any prior knowledge of that emissivity. The emissivity and its stability over time are closely associated with vegetative cover.

Our findings have significant implications for design of microwave sensors and retrieval algorithms. These findings have been applied to the design of the forthcoming Conical-scanning Microwave Imager/ Sounder (CMIS), including measurement in V and H polarization near 23 GHz and the use of cross-sensor infrared data to aid in building and maintaining a dynamic emissivity database.

Acknowledgments. This work was supported by the NPOESS Integrated Program Office under sub-contract to Boeing Satellite Systems.

REFERENCES

Bommarito, J., 1993: DMSP Special Sensor Microwave Imager Sounder (SSMIS). Proceedings, *Microwave Instrumentation for Remote Sensing of the Earth*, Orlando, FL, J. Shiue, Ed., Society of Photo-optical Instrumentation Engineers (SPIE), Bellingham, WA, 230-238.

Ferraro, R. R., F. Weng, N. C. Grody, and A. Basist, 1996: An eight-year (1987-1994) time series of rainfall, clouds, water vapor, snow cover, and sea ice derived from SSM/I measurements. *Bull. Amer. Meteor. Soc*., **77**, 891-905.

Neale, C. M. U., M. J. McFarland, and K. Chang, 1990: Land-surface-type classification using microwave brightness temperatures from the Special Sensor Microwave/Imager. *IEEE Trans. Geoscience Remote Sensing*, **28**, 829-845.

Prigent, C., W.B. Rossow, and E. Matthews, 1997: Microwave land emissivities estimated from SSM/I observations, *J. Geophys. Res*., **102**, pp 21867-21890.